Coaggregation of Paramagnetic d- and f-Block Metal Ions with a Podand-Framework Amine Phenol Ligand†

Zhiqiang Xu,‡ Paul W. Read,‡ David E. Hibbs,§ Michael B. Hursthouse,§ K. M. Abdul Malik,§ Brian O. Patrick,‡ Steven J. Rettig,‡ Mehran Seid,‡ David A. Summers,‡ Maren Pink,|| Robert C. Thompson,‡ and Chris Orvig*,‡

Medicinal Inorganic Chemistry Group, Department of Chemistry, University of British Columbia, 2036 Main Mall, Vancouver, BC V6T 1Z1, Canada, Department of Chemistry, University of Wales, Cardiff, P.O. Box 912, Cardiff CF1 3TB, U.K., and X-ray Crystallographic Laboratory, University of Minnesota, Minneapolis, Minnesota 55455

Received October 4, 1999

This report covers initial studies in the coaggregation of nickel (Ni^{2+}) and lanthanide (Ln^{3+}) metal ions to form complexes with interesting structural and magnetic properties. The tripodal amine phenol ligand H_3tam (1,1,1-tris(((2-hydroxybenzyl)amino)methyl)ethane) is shown to be particularly accommodating with respect to the geometric constraints of both transition and lanthanide metal ions, forming isolable complexes with both of these ion types. In the solid-state structure of $[Ni(H_2tam)(CH_3CN)]PF_6 \cdot 2.5CH_3CN \cdot 0.5CH_3OH$ (**1**), the Ni(II) center has a distorted octahedral geometry, with an N_3O_2 donor set from the $[H_2tam]^-$ ligand and a coordinated solvent (acetonitrile) occupying the sixth site. The reaction of stoichiometric amounts of H_3tam with the Ni(II) ion in the presence of lanthanide(III) ions provides $[LnNi_2(tam)_2]^+$ cationic complexes which contain coaggregated metal ions. These complexes are isolable and have been characterized by a variety of analytical techniques, with mass spectrometry proving to be particularly diagnostic. The solid-state structures of $[LaNi_2(tam)_2(CH_3OH)_{1/2}(CH_3CH_2OH)_{1/2}(H_2O)]ClO_4 \cdot 0.5CH_3OH \cdot 0.5CH_3CH_2OH \cdot 4H_2O$ (**2**), $[DyNi_2(tam)_2(CH_3OH)(H_2O)]ClO_4 \cdot CH_3OH \cdot H_2O$ (**6**), and $[YbNi_2(tam)_2(H_2O)]ClO_4 \cdot 2.58H_2O$ (**9**) have been determined. Each complex contains two octahedral Ni(II) ions, each of which is encapsulated by the ligand tam^{3-} in an N_3O_3 coordination sphere; each $[Ni(tam)]^-$ unit caps the lanthanide(III) ion via bridging phenoxy oxygen donor atoms. In **2**, La^{3+} is eight-coordinated, while in **6**, Dy(III) is seven- (to "weakly eight-") coordinated, and Yb(III) in **9** has a six-coordination environment. The complexes are symmetrically different, **2** possessing C_2 symmetry and **6** and **9** having C_1 symmetry. Magnetic studies of **2**, **6**, and **9** indicate that antiferromagnetic exchange coupling between the Ni(II) and Ln(III) ions increases with decreasing ionic radius of Ln(III).

Introduction

Metal complexes with high coordination numbers have received much attention for many years.[1,2] More recently, a particular area of research focus has been the chemistry of multidentate ligands with lanthanide(III) ions. This is due in part to the wide variety of uses that lanthanide(III) ions find in today's technologies; because of their magnetic and physical properties, rare earth elements are utilized as magnetic resonance imaging (MRI) contrast agents,[3,4] as ester hydrolysis reagents,[5] and in powerful magnets.[6] The magnetic properties of f-block elements is an area of research that is generating much interest and has been extensively reviewed by Kahn in a book and two review articles.[7] These writings cover in detail the magnetic properties of complexes with mixed Cu(II) and lanthanide(III) ions and hence their behavior is well studied and understood.[7] The magnetic properties of mixed Ni(II) and Ln(III) ion complexes, however, have not been previously studied in detail and have only recently been of interest.[8]

Of late, we have been investigating the reactions of amine phenol ligands with group 13 and lanthanide(III) ions in both aqueous and nonaqueous media.[9] During the course of this prior work, five different coordination modes of amine phenol ligands with lanthanide ions were structurally characterized (see Chart 1). This work has now been extrapolated to the coaggregation of d- and f-block metal ions in solution and in the solid state through encapsulation of a divalent transition metal into the bicapped structure. Amine phenol ligands are hydrolytically stable and are geometrically more flexible than their Schiff base analogues. Multidentate ligands that can incorporate two or more metal atoms are useful in studying the magnetic interactions between metal ions. Homo- and heteropolynuclear complexes

* To whom correspondence should be addressed. Tel: 604-822-4449. Fax: 604-822-2847. E-mail: orvig@chem.ubc.ca.

† This paper is dedicated to our dear friend and sadly missed colleague Steven J. Rettig.

‡ University of British Columbia.

§ University of Wales.

|| University of Minnesota.

(1) Drew, M. G. B. *Prog. Inorg. Chem.* **1977**, *23*, 67.
(2) Drew, M. G. B. *Coord. Chem. Rev.* **1977**, *24*, 179.
(3) Watson, A. D. *J. Alloys Compd.* **1994**, *207/208*, 14.
(4) Kumar, K.; Jin, T.; Wang, X.; Desreux, J. F.; Tweedle, M. F. *Inorg. Chem.* **1994**, *433*, 3823.
(5) Morrow, J. R.; Kolasa, K. A.; Amin, S.; Chin, K. O. A. *Adv. Chem. Ser.* **1995**, *246*, 431.
(6) Rauluszkiewicz, J., Szymczak, H., Lachowicz, H. K., Eds. *Physics of Magnetic Materials*; World Scientific: Singapore, 1985.
(7) (a) Kahn, O. *Struct. Bonding* (*Berlin*) **1987**, *68*, 89. (b) Kahn, O. *Adv. Inorg. Chem.* **1995**, *43*, 179. (c) Kahn, O. *Molecular Magnetism*; VCH: New York, 1993.
(8) (a) Lisowski, J.; Starynowicz, P. *Inorg. Chem.* **1999**, *38*, 1351. (b) Knoeppel, D. W.; Liu, J.; Meyers, E. A.; Shore, S. G. *Inorg. Chem.* **1998**, *37*, 4828. (c) Brechin, E. K.; Harris, S. G.; Parsons, S.; Winpenny, R. E. P. *J. Chem. Soc., Dalton Trans.* **1997**, 1665.

10.1021/ic991171b CCC: $19.00
Published on Web 01/15/2000

Chart 1

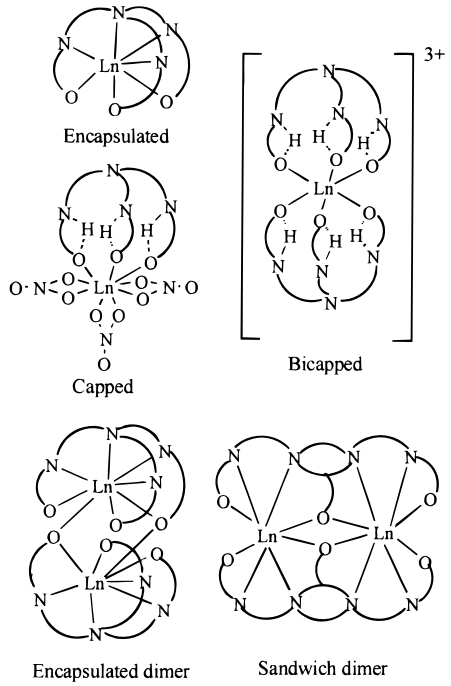

containing rare earth metals are of great interest because of their unique physicochemical properties[10] and may even be potentially useful as models of metalloenzymes and in applications to catalysis. Schiff base ligands have been used for many years to isolate polynuclear materials where the compositions and topologies of the resultant complexes can be easily controlled.[11] A systematic study has been undertaken in order to investigate the magnetophysical properties of mixed Ni_2Ln and Cu_2Ln complexes. In this paper, we present the syntheses and characterizations of a series of d- and d−f-block metal complexes of the potentially hexadentate amine phenol ligand H_3tam[12] with Ni^{2+} and Ln^{3+} ions.

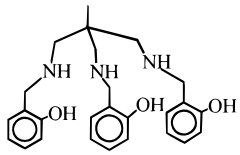

H_3tam

The choice of H_3tam as ligand in this study was not a fortuitous one, since a flexible ligand with intrinsic selectivity would favor the isolation of coaggregated metal ion complexes. The ligand H_3tam is geometrically less demanding than the Schiff base analogue saltame (1,1,1-tris(((2-hydroxybenzyl)-imino)methyl)ethane) because of the greater flexibility of the amino linkages in the amine phenol ligand. Selectivity is inherent within H_3tam, since the ligand contains (formally) both hard and soft donor atoms. The harder phenoxy O donors will bond preferentially to the hard Ln(III) ion in the absence of external factors. Transition metal ions, which are softer than Ln(III) ions, may bond preferentially to softer amine functions.

Experimental Section

Materials. $AgPF_6$ and $NiCl_2 \cdot 6H_2O$ were purchased from Aldrich. Hydrated lanthanide(III) perchlorates were obtained from Alfa either as the solid or as 50% (w/w) solutions in water, which were evaporated to dryness. Triethylamine was purchased from Fisher and was used as received. NMR solvents were purchased from Aldrich and were used as received. $Ni(ClO_4)_2 \cdot 6H_2O$ was prepared from the corresponding carbonates by dissolution in perchloric acid and H_3tam was prepared according to our literature procedure.[14] Methanol was dried prior to use over molecular sieves.

***Caution*!** *Perchlorate salts are potentially explosive and should be handled with extreme care and used only in small quantities.*[13]

Physical Measurements. ^{1}H NMR spectra (200 and 300 MHz) were recorded on Bruker AC-200E and Varian XL-300 spectrometers, respectively, and were referenced internally to residual solvent hydrogens. Mass spectra were obtained with a Kratos Concept II H32Q (Cs^+, LSIMS) instrument. Infrared spectra were recorded as KBr disks in the range 4000−400 cm^{-1} on a Mattson Galaxy Series FTIR-5000 spectrophotometer and were referenced to polystyrene (1601.3 cm^{-1}). Analyses of C, H, and N were performed by Mr. Peter Borda at the University of British Columbia. The room-temperature magnetic susceptibilities were measured on a Johnson Matthey MSB-1 balance (solid state), and variable-temperature magnetic susceptibility measurements were performed on a Quantum Design SQUID magnetometer for dried powder samples (2−300 K, 10 kG). Diamagnetic corrections were applied to the data on the basis of Pascal's constants.

Syntheses of the Complexes. (a) [Ni(H_2tam)]PF_6 (1). To a solution of $NiCl_2 \cdot 6H_2O$ (100 mg, 0.41 mmol) in methanol (5 mL) was added $AgPF_6$ (212 mg, 0.84 mmol). The solution was allowed to stir for 10 min and was then clarified by filtration. To the filtrate was added H_3-tam (183 mg, 0.42 mmol) in methanol (5 mL), and a purple color developed immediately. The solution was evaporated to ca. 2 mL, and the concentrate was allowed to stand at room temperature, whereupon purple plates deposited. The crystals were washed with a small amount of diethyl ether and dried in air. X-ray-quality crystals were obtained

(9) (a) Caravan, P.; Orvig, C. *Inorg. Chem*. **1997**, *36*, 236. (b) Lowe, M. P.; Rettig, S. J.; Orvig, C. *J. Am. Chem. Soc*. **1996**, *118*, 10446. (c) Caravan, P.; Mehrkhodavandi, P.; Orvig, C. *Inorg. Chem*. **1997**, *36*, 1316. (d) Caravan, P.; Rettig, S. J.; Orvig, C. *Inorg. Chem*. **1997**, *36*, 1306. (e) Lowe, M. P.; Caravan, P.; Rettig, S. J.; Orvig, C. *Inorg. Chem*. **1998**, *37*, 1637. (f) Wong, E.; Caravan, P.; Liu, S.; Rettig, S. J.; Orvig, C. *Inorg. Chem*. **1996**, *35*, 715. (g) Caravan, P.; Hedlund, T.; Liu, S.; Sjöberg, S.; Orvig, C. *J. Am. Chem. Soc*. **1995**, *117*, 11230. (h) Wong, E.; Liu, S.; Rettig, S. J.; Orvig, C. *Inorg. Chem*. **1995**, *34*, 3057. (i) Yang, L.-W.; Liu, S.; Wong, E.; Rettig, S. J.; Orvig, C. *Inorg. Chem*. **1995**, *34*, 2164. (j) Wong, E.; Liu, S.; Lügger, T.; Hahn, F. E.; Orvig, C. *Inorg. Chem*. **1995**, *34*, 93. (k) Liu, S.; Wang, L.-W.; Rettig, S. J.; Orvig, C. *Inorg. Chem*. **1993**, *32*, 2773. (l) Liu, S.; Gelmini, L.; Rettig, S. J.; Thompson, R. C.; Orvig, C. *J. Am. Chem. Soc*. **1992**, *114*, 6081. (m) Berg, D. J.; Rettig, S. J.; Orvig, C. *J. Am. Chem. Soc*. **1991**, *113*, 2528. (n) Smith, A.; Rettig, S. J.; Orvig, C. *Inorg. Chem*. **1988**, *27*, 3929.

(10) (a) Guerriero, P.; Vigato, P. A.; Bunzli, J.-C. G.; Moret, E. *J. Chem. Soc., Dalton Trans*. **1990**, 647. (b) Casellato, U.; Guerriero, P.; Tamburini, S.; Vigato, P. A.; Graziani, R. *J. Chem. Soc., Dalton Trans*. **1990**, 1533. (c) Guerriero, P.; Sitran, S.; Vigato, P. A.; Marega, C.; Zametti, R. *Inorg. Chim. Acta* **1990**, *171*, 103.

(11) (a) Fenton, D. E.; Okawa, H. In *Perspectives in Coordination Chemistry*; Williams, A. F., Floriani, C., Merbach, A. E., Eds.; VCH: Weinheim, Germany, 1992; p 203. (b) McKee, V. *Adv. Inorg. Chem*. **1993**, *40*, 323. (c) Nanda, K. K.; Thompson, L. K.; Brisdon, J. N.; Nag, K. *J. Chem. Soc., Chem. Commun*. **1994**, 1337. (d) Nanda, K. K.; Das, R.; Thompson, L. K.; Vewnkatsubrammanian, K.; Paul, P.; Nag, K. *Inorg. Chem*. **1994**, *33*, 1188. (e) Pilkington, N. H.; Robson, R. *Aust. J. Chem*. **1970**, *23*, 2225. (f) Atkins, A. J.; Black, D.; Blake, A. J.; Marin-Becerra, A.; Parsons, S.; Ruiz-Ramirez, L.; Schroder, M. *J. Chem. Soc., Chem. Commun*. **1996**, 457. (g) Daolio, S.; Facchin, B.; Pagura, C.; Guerriero, P.; Sitran, S.; Vigato, P. A. *Inorg. Chim. Acta* **1990**, *178*, 131. (h) Kahwa, I. A.; Selbin, J.; Hsieh, T. C.-Y.; Laine, R. A. *Inorg. Chim. Acta*, **1986**, *118*, 179. (i) Kahwa, I. A.; Fronczek, F. R.; Selbin, J. *Inorg. Chim. Acta* **1987**, *126*, 227. (j) Kahwa, I. A.; Fronczek, F. R.; Selbin, J. *Inorg. Chim. Acta* **1988**, *148*, 273. (k) Guerriero, P.; Tamburini, S.; Vigato, P. A.; Benelli, C. *Inorg. Chim. Acta* **1991**, *189*, 19.

(12) H_3tam = 1,1,1-tris(((2-hydroxybenzy)amino)methyl)ethane. The H_3 term refers to the three ionizable phenolic protons.

(13) For further information, see: Wolsey, W. C. *J. Chem. Educ*. **1973**, *50*, A335.

(14) Liu, S.; Wong, E.; Karunaratne, V.; Rettig, S. J.; Orvig, C. *Inorg. Chem*. **1993**, *32*, 1756.

Table 1. $[LnNi_2(tam)_2]ClO_4 \cdot xH_2O$ Complexes (**2**−**9**) and Their Analytical Data

complex	% C	% H	% N	$\mu_{eff/RT}$, μB	m/z of $[LnNi_2(tam)_2]^+$
$[LaNi_2(tam)_2]ClO_4 \cdot 3H_2O$ (**2**)	49.00[a]	5.24	6.70	4.05[c]	1119
	(48.99)[b]	(5.22)	(6.59)	(4.00)[d]	
$[PrNi_2(tam)_2]ClO_4 \cdot H_2O$ (**3**)	50.56	5.13	6.84	6.46[e]	1121
	(50.33)	(5.04)	(6.77)	(5.38)	
$[NdNi_2(tam)_2]ClO_4 \cdot H_2O$ (**4**)	50.20	5.17	6.73	6.72[e]	1126
	(50.20)	(5.02)	(6.75)	(5.39)	
$[GdNi_2(tam)_2]ClO_4 \cdot 3H_2O$ (**5**)	48.12	5.02	6.42	8.77[e]	1140
	(48.30)	(5.14)	(6.50)	(8.89)	
$[DyNi_2(tam)_2]ClO_4 \cdot 3H_2O$ (**6**)	47.79	4.99	6.42	11.91[c]	1144
	(48.10)	(5.12)	(6.47)	(11.33)	
$[HoNi_2(tam)_2]ClO_4 \cdot 3H_2O$ (**7**)	47.26	5.36	6.54	11.84[e]	1145
	(48.01)	(5.11)	(6.46)	(11.33)	
$[ErNi_2(tam)_2]ClO_4 \cdot 3H_2O$ (**8**)	47.43	5.26	6.63	11.05[e]	1148
	(47.92)	(5.10)	(6.45)	(10.37)	
$[YbNi_2(tam)_2]ClO_4 \cdot 3H_2O$ (**9**)	47.57	5.37	6.59	6.28[c]	1154
	(47.71)	(5.08)	(6.42)	(6.02)	

[a] Found. [b] Expected. [c] Measured on a Quantum Design SQUID magnetometer at 300 K. [d] Calculated values based on $g[J(J+1)]^{1/2}$. [e] Measured on a Johnson Matthey MSB-1 balance at room temperature.

Table 2. Crystallographic Data for Compounds **1**, **2**, **6**, and **9**

	1	**2**	**6**	**9**
empirical formula	$C_{33.5}H_{44.5}F_6N_{6.5}NiO_{3.5}P$	$C_{55}H_{54}ClLaNi_2O_{17}N_6$	$C_{54}H_{69}ClDyN_6Ni_2O_{14}$	$C_{53}H_{73.16}ClN_6Ni_2O_{15.58}Yb$
fw	797.94	1362.82	1341.52	1369.52
space group	*C*2/*c* (No. 15)	*C*2/*c* (No. 15)	*C*2/*c* (No. 15)	$P2_1/c$(No. 14)
a, Å	25.296(7)	31.731(3)	31.9836(9)	14.9263(7)
b, Å	16.163(6)	23.491(3)	22.2077(9)	18.5192(10)
c, Å	20.367(8)	19.868(2)	20.1328(2)	22.5309(2)
α, deg	90.0	90	90.0	90.0
β, deg	105.30(2)	124.924(6)	123.7124(2)	92.5859(2)
γ, deg	90.0	90	90.0	90.0
V, Å^3	8032(5)	12143(2)	11895.2(4)	6221.7(3)
Z	8	4	8	4
ρ_{obsd}, mg m^{-3}	1.320	0.745	1.498	1.462
T, (*K*)	150(1)	173(2)	180(1)	180(1)
λ, Å	0.710 69	0.710 73	0.710 69	0.710 69
μ, mm^{-1}	0.592	0.710	1.983	2.199
R1[a]	0.0616	0.0451	0.045	0.046
wR2[a]	0.1645[b]	0.1156[b]	0.099[c]	0.087[c]

[a] R1 and wR2 as defined in SHELX-93. [b] $w = 1/[\sigma^2(F_o^2) + (0.0827P)^2]$, where $P = (F_o^2 + 2F_c^2)/3$. [c] $w = 1/[\sigma^2(F_o^2) + (0.0322P)^2]$, where $P = (F_o^2 + 2F_c^2)/3$.

from CH_3CN. Yield: 210 mg (80%). Anal. Calcd (found) for $C_{26}H_{32}F_6N_3NiO_3P$: C, 48.93 (48.88); H, 5.05 (5.15); N, 6.58 (6.41). $\mu_{eff}(RT) = 3.04\ \mu_B$. Mass spectrum (LSIMS): m/z 492 ($[Ni(H_2tam)]^+$, $C_{26}H_{32}N_3NiO_3^+$), 983 ($[Ni_2(H_2tam)_2 - H]^+$, $C_{52}H_{63}N_6Ni_2O_6^+$). IR (cm^{-1}; KBr disk): 3472 (m, vbr), 3272 (s, s), 3056 (w, s), 2934 (w, s), 2907 (w, s), 2861 (w, s), 1598 (s, s), 1479 (s, s), 1378 (w, s), 1352 (w, s), 1278 (m, s), 1241 (w, s), 918 (m, s), 897 (m, s), 873 (m, s), 840 (m, s), 764 (m, s), 745 (m, s), 734 (w, s), 622 (s, s), 572 (m, s), 566 (m, s), 555 (w, s).

(b) General Procedure for $[LnNi_2(tam)_2]ClO_4 \cdot nH_2O$ (2−9). To a solution of $Ni(ClO_4)_2 \cdot 6H_2O$ (100 mg, 0.27 mmol) in methanol (5 mL) was added H_3tam (120 mg, 0.28 mmol) in methanol (5 mL). The blue solution was left to stir at room temperature for 10 min, and hydrated $Ln(ClO_4)_3 \cdot xH_2O$ then was added (0.13 mmol). The solution developed a light red hue (for all Ln complexes) and upon addition of triethylamine (84 mg, 0.83 mmol) became more intensely colored. The solution was allowed to stand for a few hours, and then 1.5 mL of deionized water was added. The resulting clear solution was clarified by filtration, and the filtrate was allowed to stand at room temperature. Light-pink (for all Ln complexes) crystals suitable for crystallographic study were formed; these were stable in the parent solvent and lost coordinated (via MeOH−H_2O exchange in parent solution) or lattice MeOH in air. The yields of the air-dried products were 40−71%. The compounds prepared and their analytical data are presented in Table 1. IR (cm^{-1}; KBr disk) (all superimposable): 3442 (s, vbr), 3272 (s, s), 3058 (w, s), 2914 (m, s), 1594 (s, s), 1566 (w, s), 1478 (s, s), 1456 (s, s), 1355 (w, s), 1281 (s, s), 995 (m, s), 920 (w, s), 896 (s, s), 878 (s, s), 854 (w, s), 759 (m, s), 734 (w, s), 630 (m, s), 591 (m, s), 515 (w, s).

X-ray Crystallographic Data Collections and Refinements of the Structures. Selected crystallographic data for complexes **1**, **2**, **6**, and **9** are presented in Table 2. The data collection for **1** was undertaken at 150 K, while those for **2**, **6**, and **9** were performed at 180 K.

(a) $[Ni(H_2tam)]PF_6$ (1). Data collection for **1** was accomplished at the University of Wales with a Delft Instruments FAST TV area detector diffractometer positioned at the window of a rotating-anode generator. Mo Kα radiation ($\lambda = 0.710\ 69$ Å) was used, and previously described procedures were followed.[15] The structure was solved by direct methods (SHELXS)[16a] and refined on F^2 by full-matrix least-squares procedures (SHELX-93)[16b] using all unique F^2 data corrected for Lorentz and polarization factors and for absorption effects (DIFABS) (absorption correction factors 0.872−0.987).[16c]

Compound **1** contained a CH_3CN molecule coordinated to Ni and 2.5 CH_3CN and 0.5 CH_3OH molecules (per complex cation) in the lattice. Both lattice components were disordered and partially occupied. There were two PF_6^- anions, each sited on 2-fold axes, thus generating a total of one PF_6^- anion per complex cation. The hydrogen atoms on

(15) Drake, S. R.; Hursthouse, M. B.; Malik, K. M. A.; Miller, S. A. S. *Inorg. Chem.* **1993**, *32*, 5704.

(16) (a) Sheldrick, G. M. *Acta Crystallogr., Sect. A* **1990**, *46*, 467. (b) Sheldrick, G. M. *SHELX-93*: *Program for Crystal Structure Refinement*; University of Göttingen: Göttingen, Germany, 1993. (c) Walker, N. P. C.; Stuart, D. *Acta Crystallogr., Sect. A* **1983**, *39*, 158. Adapted for FAST geometry by A. Karaulov, University of Wales, Cardiff, 1991.

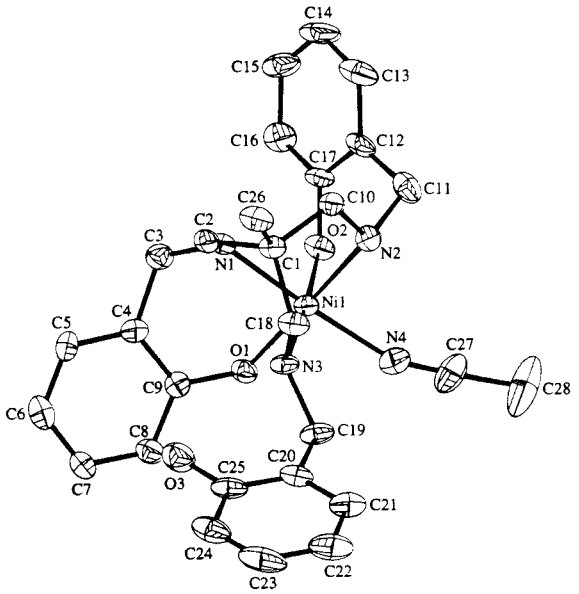

Figure 1. Structure of the $[Ni(H_2tam)(CH_3CN)]^+$ cation in **1**. Thermal ellipsoids are drawn at 50% probability, and hydrogen atoms are omitted for clarity.

Table 3. Selected Bond Lengths (Å) and Angles (deg) for the $[Ni(H_2tam)]^+$ Cation in **1**

Ni(1)−O(2)	2.035(3)	Ni(1)−N(4)	2.075(5)
Ni(1)−N(1)	2.077(4)	Ni(1)−O(1)	2.078(3)
Ni(1)−N(2)	2.083(4)	Ni(1)−N(3)	2.111(4)
O(2)−Ni(1)−N(4)	88.8(2)	O(2)−Ni(1)−N(1)	88.9(2)
N(4)−Ni(1)−N(1)	176.1(2)	O(2)−Ni(1)−O(1)	87.97(13)
N(4)−Ni(1)−O(1)	91.5(2)	N(1)−Ni(1)−O(1)	91.5(2)
O(2)−Ni(1)−N(2)	91.3(2)	N(4)−Ni(1)−N(2)	89.2(2)
N(1)−Ni(1)−N(2)	87.7(2)	O(1)−Ni(1)−N(2)	179.00(14)
O(2)−Ni(1)−N(3)	175.5(2)	N(4)−Ni(1)−N(3)	95.2(2)
N(1)−Ni(1)−N(3)	87.3(2)	O(1)−Ni(1)−N(3)	89.8(2)
N(2)−Ni(1)−N(3)	90.8(2)	C(9)−O(1)−Ni(1)	121.9(3)

the phenolic O(1) and CH_3OH solvate were ignored; others were included in calculated positions (riding model). All non-hydrogen atoms were refined with anisotropic displacement coefficients, with those for the acetonitrile species being restrained using an ISOR 0.01 instruction in SHELX-93. The C−N and C−C distances in the acetonitrile molecules were also restrained to refine to the same group values. Selected distances and angles are shown in Table 3, and an ORTEP drawing of the complex cation is presented in Figure 1.

(b) $[LaNi_2(tam)_2(CH_3OH)_{1/2}(CH_3CH_2OH)_{1/2}(H_2O)]ClO_4\cdot 0.5CH_3OH\cdot 0.5CH_3CH_2OH\cdot 4H_2O$ (2). Data collection for **2** was undertaken at the University of Minnesota. A violet crystal of approximate dimensions $0.13 \times 0.13 \times 0.07$ mm^3 was attached to the tip of a 0.1 mm diameter glass capillary, which was then mounted on a Siemens SMART system for data collection at 173(2) K. The data collection was carried out using Mo Kα radiation (graphite monochromator) with a detector distance of 4.934 cm. A randomly oriented region of reciprocal space was surveyed to the extent of 1.3 hemispheres and to a resolution of 0.84 Å. Three major sections of frames were collected with 0.30° steps in ω at three different ϕ settings and a detector position of −25° in 2θ with a frame time of 30 s. Selected distances and angles are shown in Table 4, and an ORTEP drawing of the complex cation is presented in Figure 2.

The structure was solved and refined using SHELX-86 and SHELX-97.[17] The space group *C*2/*c* was determined on the basis of systematic absences and intensity statistics. The heavy-atom positions were determined from a Patterson solution. Full-matrix least-squares/difference Fourier cycles were performed, locating the remaining non-hydrogen atoms of the cationic complex and the perchlorate anion (site occupancy $^1/_2$, located on an inversion center). However, the location of the remaining half of the anion and solvent molecules was not determinable due to the large voids in the unit cell. These voids allowed for disordered solvent molecules and made it necessary to correct the data using PLATON.[18] The voids are situated in the vicinity of a disordered oxygen, O(8)/O(8d), belonging 67% of the time to an alcohol and 33% of the time to water. All non-hydrogen atoms were refined with anisotropic displacement parameters except for those of half of a perchlorate (Cl(2), ...). The hydrogen atoms were placed in ideal positions and refined as riding atoms with individual or group isotropic displacement parameters or were found from the *E* map. The final full-matrix least-squares refinement converged to R1 = 0.0451 and wR2

Table 4. Selected Bond Lengths (Å) and Angles (deg) for the $[LaNi_2(tam)_2(CH_3OH)_{1/2}(CH_3CH_2OH)_{1/2}(H_2O)]^+$ Cation in **2**

La(1)−Ni(1)	3.1900(7)	La(1)−Ni(2)	3.1533(7)
La(1)−O(1)	2.449(3)	La(1)−O(2)	2.472(3)
La(1)−O(3)	2.450(3)	La(1)−O(4)	2.410(3)
La(1)−O(5)	2.455(3)	La(1)−O(6)	2.496(3)
La(1)−O(7)	2.638(3)	La(1)−O(8)	2.683(10)
La(1)−O(8d)	2.62(2)	Ni(1)−O(1)	2.101(3)
Ni(1)−O(2)	2.050(3)	Ni(1)−O(3)	2.075(3)
Ni(1)−N(1)	2.075(4)	Ni(1)−N(2)	2.078(3)
Ni(1)−N(3)	2.093(4)	Ni(2)−O(4)	2.089(3)
Ni(2)−O(5)	2.085(3)	Ni(2)−O(6)	2.061(3)
Ni(2)−N(4)	2.081(4)	Ni(2)−N(5)	2.092(4)
Ni(2)−N(6)	2.069(4)		
Ni(1)−La(1)−O(6)	165.30(8)	Ni(1)−La(1)−O(7)	112.01(12)
Ni(1)−La(1)−O(8)	99.7(3)	Ni(1)−La(1)−O(8d)	100.9(4)
Ni(2)−La(1)−O(1)	126.69(8)	Ni(2)−La(1)−O(2)	105.68(8)
Ni(2)−La(1)−O(3)	160.93(8)	Ni(2)−La(1)−O(4)	41.47(7)
Ni(2)−La(1)−O(5)	41.35(7)	Ni(2)−La(1)−O(6)	40.75(7)
Ni(2)−La(1)−O(7)	97.80(11)	Ni(2)−La(1)−O(8)	108.8(3)
Ni(2)−La(1)−O(8d)	113.0(6)	O(1)−La(1)−O(2)	68.66(10)
O(1)−La(1)−O(3)	69.09(11)	O(1)−La(1)−O(4)	145.80(11)
O(1)−La(1)−O(5)	86.14(11)	O(1)−La(1)−O(6)	124.15(11)
O(1)−La(1)−O(7)	132.28(14)	O(1)−La(1)−O(8)	73.0(7)
O(1)−La(1)−O(8d)	82.3(8)	O(2)−La(1)−O(3)	67.96(11)
O(2)−La(1)−O(4)	83.76(10)	O(2)−La(1)−O(5)	84.31(11)
O(2)−La(1)−O(6)	146.34(10)	O(2)−La(1)−O(7)	119.4(2)
O(2)−La(1)−O(8)	138.8(4)	O(2)−La(1)−O(8d)	140.7(4)
O(3)−La(1)−O(4)	119.55(11)	O(3)−La(1)−O(5)	147.79(11)
O(3)−La(1)−O(6)	143.90(11)	O(3)−La(1)−O(7)	71.97(14)
O(3)−La(1)−O(8)	85.1(4)	O(3)−La(1)−O(8d)	77.4(9)
O(4)−La(1)−O(5)	70.87(11)	O(4)−La(1)−O(6)	70.38(10)
O(4)−La(1)−O(7)	78.56(14)	O(4)−La(1)−O(8)	137.4(5)
O(4)−La(1)−O(8d)	131.1(7)	O(5)−La(1)−O(6)	67.33(11)
O(5)−La(1)−O(7)	138.91(13)	O(5)−La(1)−O(8)	107.7(7)
O(5)−La(1)−O(8d)	120.6(14)	O(6)−La(1)−O(7)	77.04(14)
O(6)−La(1)−O(8)	70.3(3)	O(6)−La(1)−O(8d)	72.3(6)
O(7)−La(1)−O(8)	77.3(9)	O(7)−La(1)−O(8d)	63.0(14)
La(1)−Ni(1)−O(1)	50.13(8)	La(1)−Ni(1)−O(2)	50.80(9)
La(1)−Ni(1)−O(3)	50.19(9)	La(1)−Ni(1)−N(1)	125.09(11)
La(1)−Ni(1)−N(2)	126.09(11)	La(1)−Ni(1)−N(3)	125.71(11)
O(1)−Ni(1)−O(2)	83.92(13)	O(1)−Ni(1)−O(3)	83.42(13)
O(1)−Ni(1)−N(1)	92.19(14)	O(1)−Ni(1)−N(2)	93.66(14)
O(1)−Ni(1)−N(3)	175.35(14)	O(2)−Ni(1)−O(3)	83.68(13)
O(2)−Ni(1)−N(1)	175.71(14)	O(2)−Ni(1)−N(2)	93.72(14)
O(2)−Ni(1)−N(3)	94.4(2)	O(3)−Ni(1)−N(1)	94.10(14)
O(3)−Ni(1)−N(2)	176.27(14)	O(3)−Ni(1)−N(3)	92.1(2)
N(1)−Ni(1)−N(2)	88.3(2)	N(1)−Ni(1)−N(3)	89.3(2)
N(2)−Ni(1)−N(3)	90.8(2)	La(1)−Ni(2)−O(4)	49.82(8)
La(1)−Ni(2)−O(5)	51.07(9)	La(1)−Ni(2)−O(6)	52.24(9)
La(1)−Ni(2)−N(4)	124.47(10)	La(1)−Ni(2)−N(5)	127.08(10)
La(1)−Ni(2)−N(6)	123.56(10)	O(4)−Ni(2)−O(5)	85.02(13)
O(4)−Ni(2)−O(6)	85.90(13)	O(4)−Ni(2)−N(4)	91.94(13)
O(4)−Ni(2)−N(5)	176.53(13)	O(4)−Ni(2)−N(6)	91.29(13)
O(5)−Ni(2)−O(6)	82.91(13)	O(5)−Ni(2)−N(4)	94.38(14)
O(5)−Ni(2)−N(5)	91.6(2)	O(5)−Ni(2)−N(6)	174.60(14)
O(6)−Ni(2)−N(4)	176.67(13)	O(6)−Ni(2)−N(5)	92.8(2)
O(6)−Ni(2)−N(6)	92.90(14)	N(4)−Ni(2)−N(5)	89.2(2)
N(4)−Ni(2)−N(6)	89.7(2)	N(5)−Ni(2)−N(6)	92.0(2)

(17) *SHELXTL-Plus V5.1*; Bruker-AXS: Madison, WI, 1998.

(18) Spek, A. L. PLATON: *Acta Crystallogr., Sect. A* **1990**, *A46*, 34.

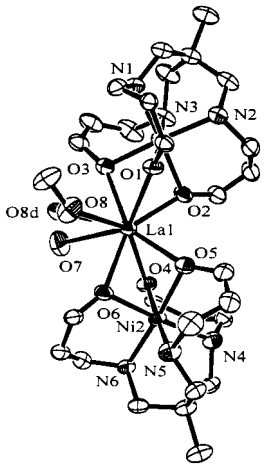

Figure 2. Structure of the $[LaNi_2(tam)_2(CH_3OH)_{1/2}(CH_3CH_2OH)_{1/2}(H_2O)]^+$ cation in **2**. Thermal ellipsoids are drawn at 50% probability, and hydrogen and ring carbon atoms are omitted for clarity.

= 0.1213 (F^2, all data). The modified dataset improved the R1 value by approximately 1.5%.

(c) $[DyNi_2(tam)_2(CH_3OH)(H_2O)]ClO_4 \cdot CH_3OH \cdot H_2O$ (6) and $[YbNi_2(tam)_2(H_2O)]ClO_4 \cdot 2.58H_2O$ (9). These structures were determined at the University of British Columbia. A pink (dark) prism crystal of complex **6** (**9**) was mounted on a glass fiber. All measurements were made on a Rigaku/ADSC CCD area detector with graphite-monochromated Mo Kα radiation. The data were collected at a temperature of 180 ± 1 K to a maximum 2θ value of 61.1° (61.0°) and at 0.30° oscillations with 10.0 s (20.0 s) exposures. A sweep of data was performed using ϕ oscillations from −23.0 to +17.8° at $\chi = -90°$ (+89.9°), and a second sweep was performed using ω oscillations between 0 and 180° at $\chi = -90°$. The structures were solved by the heavy-atom Patterson method[19] and expanded using Fourier techniques.[20] In **6**, there is half of a perchlorate ion disordered about a center of symmetry. The other perchlorate could not be located and most likely resides, along with disordered methanol and water, in the primary solvent region. All calculations were performed using the teXsan[21] crystallographic software package.

Selected distances and angles are shown in Tables 5 and 6 for compounds **6** and **9**, respectively, while ORTEP drawings of the complex cations in **6** and **9** are presented in Figures 3 and 4, respectively.

Full details of the structure solutions for **1**, **2**, **6**, and **9**, as well as complete tables of crystallographic data, atomic coordinates and equivalent isotropic thermal parameters, hydrogen atom parameters, anisotropic thermal parameters, bond lengths, bond angles, torsion angles, intermolecular contacts, and least-squares planes, are included as Supporting Information.

Results and Discussion

Structures. To evaluate the ability of the H_3tam ligand to coaggregate d- and f-block metal ions, it was first necessary to study the reactions of the ligand with Ni^{2+} alone. The isolation of a $Ni^{2+}-H_3$tam binary complex was important to this study because it is the building block from which the larger coaggregated LnM_2 complexes are formed.

Table 5. Selected Bond Lengths (Å) Angles (deg) for the $[DyNi_2(tam)_2(CH_3OH)(H_2O)]^+$ Cation in **6**

Dy(1)−Ni(1)	3.0134(7)	Dy(1)−Ni(2)	3.2542(7)
Dy(1)−O(1)	2.268(3)	Dy(1)−O(2)	2.273(4)
Dy(1)−O(3)	2.286(4)	Dy(1)−O(4)	2.267(3)
Dy(1)−O(5)	2.257(3)	Dy(1)−O(7)	2.398(4)
Ni(1)−O(1)	2.082(4)	Ni(1)−O(2)	2.061(3)
Ni(1)−O(3)	2.055(4)	Ni(1)−N(1)	2.063(4)
Ni(1)−N(2)	2.072(4)	Ni(1)−N(3)	2.053(3)
Ni(2)−O(4)	2.080(4)	Ni(2)−O(5)	2.095(3)
Ni(2)−O(6)	2.070(4)	Ni(2)−N(4)	2.091(4)
Ni(1)−N(5)	2.098(5)	Ni(2)−N(6)	2.056(5)
O(1)−C(6)	1.342(6)	O(2)−C(14)	1.329(6)
O(3)−C(22)	1.339(6)	O(4)−C(32)	1.342(6)
O(5)−C(35)	1.355(6)	O(6)−C(48)	1.330(6)
O(1)−Dy(1)−O(2)	74.55(12)	O(1)−Dy(1)−O(3)	72.63(12)
O(1)−Dy(1)−O(4)	163.81(13)	O(1)−Dy(1)−O(5)	119.36(12)
O(1)−Dy(1)−O(7)	105.23(12)	O(1)−Dy(1)−O(8)	75.56(13)
O(2)−Dy(1)−O(3)	71.10(12)	O(2)−Dy(1)−O(4)	90.37(12)
O(2)−Dy(1)−O(5)	154.93(14)	O(2)−Dy(1)−O(7)	76.66(13)
O(2)−Dy(1)−O(8)	129.03(14)	O(3)−Dy(1)−O(4)	97.22(13)
O(3)−Dy(1)−O(5)	92.36(13)	O(3)−Dy(1)−O(7)	147.08(14)
O(3)−Dy(1)−O(8)	134.60(13)	O(4)−Dy(1)−O(5)	72.68(12)
O(4)−Dy(1)−O(7)	76.22(13)	O(4)−Dy(1)−O(8)	119.56(13)
O(5)−Dy(1)−O(7)	115.40(13)	O(5)−Dy(1)−O(8)	76.00(15)
O(7)−Dy(1)−O(8)	72.66(15)	O(1)−Ni(1)−O(2)	83.19(14)
O(1)−Ni(1)−O(3)	81.39(15)	O(1)−Ni(1)−N(1)	92.04(15)
O(1)−Ni(1)−N(2)	94.5(2)	O(1)−Ni(1)−N(3)	174.44(15)
O(2)−Ni(1)−O(3)	80.19(14)	O(2)−Ni(1)−N(1)	175.0(2)
O(2)−Ni(1)−N(2)	92.66(15)	O(2)−Ni(1)−N(3)	92.85(15)
O(3)−Ni(1)−N(1)	97.5(2)	O(3)−Ni(1)−N(2)	172.10(15)
O(3)−Ni(1)−N(3)	94.1(2)	N(1)−Ni(1)−N(2)	89.3(2)
N(1)−Ni(1)−N(3)	91.8(2)	N(2)−Ni(1)−N(3)	89.6(2)
O(4)−Ni(2)−O(5)	79.90(13)	O(4)−Ni(1)−O(6)	88.33(14)
O(4)−Ni(2)−N(4)	91.87(15)	O(4)−Ni(2)−N(5)	92.4(2)
O(4)−Ni(2)−N(6)	175.79(14)	O(5)−Ni(2)−O(6)	90.26(14)
O(5)−Ni(2)−N(4)	171.4(2)	O(5)−Ni(2)−N(5)	90.08(14)
O(5)−Ni(2)−N(6)	95.99(14)	O(6)−Ni(2)−N(4)	91.97(15)
O(6)−Ni(2)−N(5)	179.3(2)	O(6)−Ni(2)−N(6)	91.97(15)
N(4)−Ni(2)−N(5)	87.8(2)	N(4)−Ni(2)−N(6)	92.3(2)
N(5)−Ni(2)−N(6)	88.5(2)		

(a) $[Ni(H_2tam)(CH_3CN)]PF_6$ (1). The room-temperature addition of H_3tam to methanolic solutions of $NiX_2 \cdot 6H_2O$ ($X = Cl^-, NO_3^-, PF_6^-, ClO_4^-, BPh_4^-$) afforded purple solutions from which materials of stoichiometry $[Ni(H_2tam)]X$ were isolated in moderate to good yields. These materials were soluble in alcohols and acetonitrile, and their elemental analyses confirmed the proposed general stoichiometry. If, however, the reaction mixtures were allowed to stand for longer periods of time (>2 h; $X = Cl^-, NO_3^-, ClO_4^-$), precipitates formed that had the same mass analysis as **1**, but a dimeric structure in the solid state, for instance, $[Ni_2(H_2tam)_2Cl]Cl$, which was structurally characterized but could not be refined to a publishable level.[22] $[Ni(H_2tam)]PF_6$ had a room-temperature solid-state magnetic moment of 3.04 μ_B, which is consistent with a d^8 octahedral species.

The structure of the cation $[Ni(H_2tam)(CH_3CN)]^+$ as its PF_6 salt is shown in Figure 1, while selected bond lengths and angles in the cation are presented in Table 3. The solid-state structure of **1** revealed that the Ni(II) ion has an octahedral geometry, its coordination sphere defined by one phenolato, one phenol, and three amine functions from the ligand $[H_2tam]^-$. The sixth site is occupied by a CH_3CN solvent molecule. The coordination environment is best described as a distorted octahedron. The third ligand phenol OH is neither deprotonated nor coordinated to the Ni center. In this complex, the Ni(II) center has a greater preference for the three amine functions versus the three phenol

(19) Beurskens, P. T.; Admiraal, G.; Beurskens, G.; Bosman, W. P.; Garcia-Granda, S.; Gould, R. O.; Smits, J. M. M.; Smykalla, C. PATTY. In *The DIRDIF program system*; Technical Report; Crystallography Laboratory, University of Nijmegen: Nijmegen, The Netherlands, 1992.

(20) Beurskens, P. T.; Admiraal, G.; Beurskens, G.; Bosman, W. P.; de Gelder, R.; Israel, R.; Smits, J. M. M. *The DIRDIF-94 program system*; Technical Report; Crystallography Laboratory, University of Nijmegen: Nijmegen, The Nertherlands, 1994.

(21) *teXsan: Crystal Structure Analysis Package*; Molecular Structure Corp.: The Woodlands, TX, 1985 and 1992.

(22) Read, P. W.; Yap, G.; Orvig, C. Unpublished results.

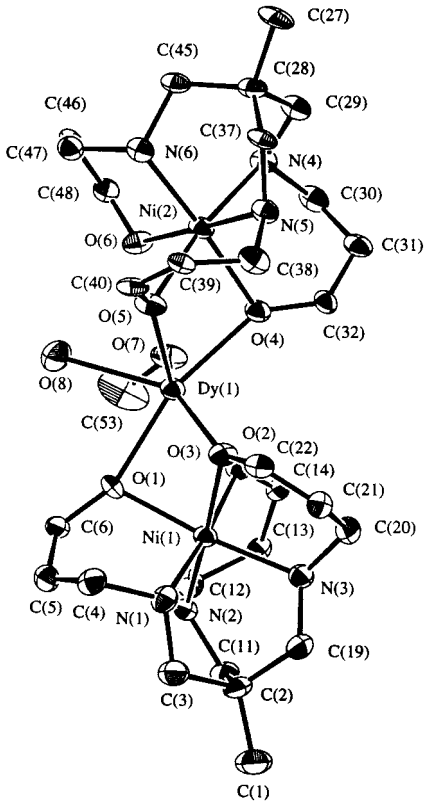

Figure 3. Structure of the $[DyNi_2(tam)_2(CH_3OH)(H_2O)]^+$ cation in **6**. Thermal ellipsoids are drawn at 50% probability, and hydrogen and ring carbon atoms are omitted for clarity.

Table 6. Selected Bond Lengths (Å) and Angles (deg) for the $[YbNi_2(tam)_2]^+$ Cation in **9**

Yb(1)−Ni(1)	2.9081(8)	Yb(1)−Ni(2)	3.2702(7)
Yb(1)−O(1)	2.207(3)	Yb(1)−O(2)	2.205(3)
Yb(1)−O(3)	2.224(4)	Yb(1)−O(4)	2.184(4)
Yb(1)−O(5)	2.176(3)	Yb(1)−O(7)	2.228(4)
Ni(1)−O(1)	2.066(4)	Ni(1)−O(2)	2.095(4)
Ni(1)−O(3)	2.098(3)	Ni(1)−N(1)	2.054(4)
Ni(1)−N(2)	2.045(6)	Ni(1)−N(3)	2.053(3)
Ni(2)−O(4)	2.126(4)	Ni(2)−O(5)	2.124(4)
Ni(2)−O(6)	2.019(4)	Ni(2)−N(4)	2.093(5)
Ni(2)−N(5)	2.083(5)	Ni(1)−N(6)	2.082(4)
O(1)−Yb(1)−O(2)	77.78(12)	O(1)−Yb(1)−O(3)	75.77(14)
O(1)−Yb(1)−O(4)	172.49(13)	O(1)−Yb(1)−O(5)	99.31(12)
O(1)−Yb(1)−O(7)	95.94(14)	O(2)−Yb(1)−O(3)	75.83(14)
O(2)−Yb(1)−O(4)	104.97(13)	O(2)−Yb(1)−O(5)	175.03(14)
O(2)−Yb(1)−O(7)	94.14(14)	O(3)−Yb(1)−O(4)	97.97(14)
O(3)−Yb(1)−O(5)	99.61(13)	O(3)−Yb(1)−O(7)	168.03(12)
O(4)−Yb(1)−O(5)	77.43(13)	O(4)−Yb(1)−O(7)	90.86(14)
O(5)−Yb(1)−O(7)	90.16(14)	O(1)−Ni(1)−O(2)	83.50(14)
O(1)−Ni(1)−O(3)	81.62(14)	O(1)−Ni(1)−N(1)	93.1(2)
O(1)−Ni(1)−N(2)	175.1(2)	O(1)−Ni(1)−N(3)	92.7(2)
O(2)−Ni(1)−O(3)	80.96(14)	O(2)−Ni(1)−N(1)	95.9(2)
O(2)−Ni(1)−N(2)	92.0(2)	O(2)−Ni(1)−N(3)	171.67(15)
O(3)−Ni(1)−N(1)	174.1(2)	O(3)−Ni(1)−N(2)	95.7(2)
O(3)−Ni(1)−N(3)	91.2(2)	N(1)−Ni(1)−N(2)	89.4(2)
N(1)−Ni(1)−N(3)	91.7(2)	N(2)−Ni(1)−N(3)	91.5(2)
O(4)−Ni(2)−O(5)	79.81(14)	O(4)−Ni(1)−O(6)	89.93(14)
O(4)−Ni(2)−N(4)	90.2(2)	O(4)−Ni(2)−N(5)	172.3(2)
O(4)−Ni(2)−N(6)	97.3(2)	O(5)−Ni(2)−O(6)	90.38(14)
O(5)−Ni(2)−N(4)	91.1(2)	O(5)−Ni(2)−N(5)	92.5(2)
O(5)−Ni(2)−N(6)	176.4(2)	O(6)−Ni(2)−N(4)	178.5(2)
O(6)−Ni(2)−N(5)	90.0(2)	O(6)−Ni(2)−N(6)	91.8(2)
N(4)−Ni(2)−N(5)	90.0(2)	N(4)−Ni(2)−N(6)	86.7(2)
N(5)−Ni(2)−N(6)	90.4(2)		

groups. Once this preference has been indulged, the strain within the molecule prevents $[H_2tam]^-$ from becoming hexadentate.[23]

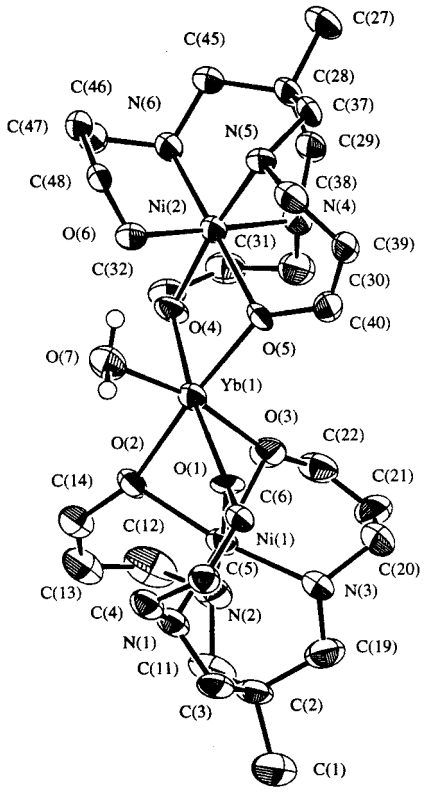

Figure 4. Structure of the $[YbNi_2(tam)_2]^+$ cation in **9**. Thermal ellipsoids are drawn at 50% probability, and hydrogen and ring carbon atoms are omitted for clarity.

The average Ni−O and Ni−N bond lengths (2.056(3) and 2.086(5) Å, respectively) are in good agreement with previous literature examples [e.g., Ni−O = 2.08 Å in $[NiL_3]^{2+}$ (L = $HOCH_2CH_2NH_2$)[24a,b] and Ni−N = 2.05 Å in $Ni[L_2]^{2+}$ (L = $H_2NCH_2CH_2)_2NH$)[24c]], although the Ni−N bond lengths are shorter than expected for six-membered chelate rings, which are typically around 2.22 Å.[24d] The Ni−acetonitrile Ni(1)−N(4) bond length (2.075(5) Å) also agrees with literature values.[25] One of the Ni−O bonds is 0.043 Å shorter than the other (Ni(1)−O(2) = 2.035(3) Å versus Ni(1)−O(1) = 2.078(3) Å), and therefore, O(2) is tentatively assigned as the deprotonated phenolato function. It is interesting to note that there is a lengthening of the Ni−N bond trans to the deprotonated phenolato O(2) (Ni(1)−N(3) = 2.111(4) Å) relative to that trans to the protonated phenol function O(1) (Ni(1)−N(2) = 2.083(4) Å). This is probably attributable to the different trans influence of a coordinated phenol OH versus a phenolato O^- function. It is unlikely to be a consequence of chelate strain within the molecule, since N(3) is only involved in two six-membered chelate rings with the Ni center (with N(1) and N(2)), whereas both N(1) and N(2) are involved in three chelate rings: N(2), N(3), O(1) and N(1), N(3), O(2), respectively. All chelate rings within the complex are six membered, and these impart a lower stability than do five-membered chelate rings. Thus, N(3) should be able to attain a closer Ni interaction since

(23) Stephens, A. K. W.; Orvig, C. *J. Chem. Soc., Dalton Trans.* **1998**, 3049.

(24) (a) Bertrand, J. A.; Howard, W. J.; Kalyararaman, A. R. *J. Chem. Soc., Chem. Commun.* **1971**, 437. (b) Rastorgi, S. C.; Rao, G. N. *J. Inorg. Nucl. Chem.* **1974**, *36*, 161. (c) Biagini, S.; Cannas, M. *J. Chem. Soc. A* **1970**, 2398. (d) Vacca, A.; Arenare, D.; Paoletti, P. *Inorg. Chem.* **1966**, *5*, 1384.

(25) Sotofte, S.; Gronbaer, R.; Rasmussen, S. E. *Acta Crystallogr., Sect. B* **1968**, *87*, 513.

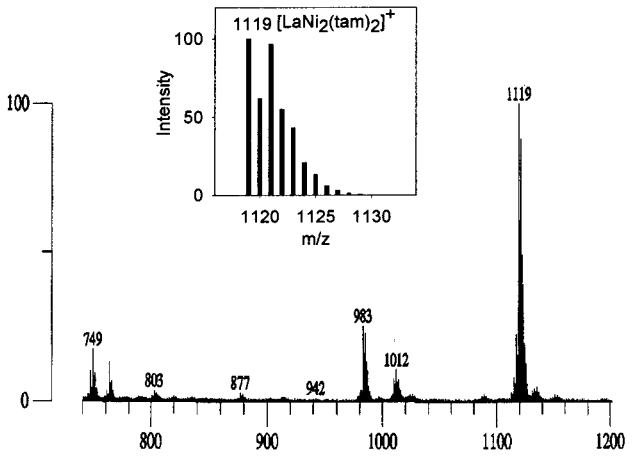

Figure 5. Mass spectrum (LSIMS) of $[LaNi_2(tam)_2]^+$ (insert: calculated parent peak).

it is less sterically encumbered and less destabilized by being in an unfavorably sized chelate ring.

Also present in the unit cell are the PF_6^- counterion and 2.5 acetonitrile and 0.5 methanol disordered solvate molecules. Two PF_6^- moieties are present in the unit cell, each sitting on a 2-fold axis, generating one PF_6^- per cation.

(b) $[LnNi_2(tam)_2]ClO_4 \cdot nH_2O$ (2−9). The $[Ni(H_2tam)]^+$ (vide infra) moiety can be deprotonated and used as an encapsulated ligand for a variety of Ln(III) ions in a bicapped fashion (see Chart 1) to generate isolable complexes which are the result of a spontaneous self-assembly: $[LnNi_2(tam)_2]^+$ (Ln = La, Pr, Nd, Gd, Dy, Ho, Er, Yb) cations.

The reaction of methanolic solutions of $[Ni(H_2tam)]ClO_4$ with hydrated lanthanide(III) perchlorate salts in the presence of base (NEt_3) afforded purple solutions, from which crystals of the corresponding lanthanide complexes (Table 1) could be isolated in moderate to good yields. The amount of base added to the reaction mixtures was important; if even slight excesses were employed, complexes of the stoichiometry indicated could not be isolated. Microanalyses confirmed the proposed stoichiometry, and LSIMS mass spectrometry was particularly diagnostic for the presence of the appropriate $[LnNi_2(tam)_2]^+$ moiety in each complex (Figure 5). IR studies showed that the complexes had initially superimposable spectra, suggesting that in the solid state all complexes had similar structures. The complexes prepared and their analytical data are presented in Table 1; they were all paramagnetic in the solid state.

Reasonably good single crystals of **2**−**9** were obtained; however, only three of these $[LnNi_2(tam)_2]^+$ complexes were structurally elucidated by X-ray diffraction [Ln = La (**2**), Dy (**6**), Yb (**9**)]. In most cases, the single crystals were obtained from the parent solvent; some, however, were obtained in purer form by recrystallization from a methanol/water mixed solvent (5:1).

(c) $[LaNi_2(tam)_2(CH_3OH)_{1/2}(CH_3CH_2OH)_{1/2}(H_2O)]ClO_4 \cdot 0.5CH_3OH \cdot 0.5CH_3CH_2OH \cdot 4H_2O$ (2). The structure of the cation $[LaNi_2(tam)_2(CH_3OH)_{1/2}(CH_3CH_2OH)_{1/2}(H_2O)]^+$ in **2** is depicted in Figure 2, where the carbon atoms in the ligand phenyl rings are omitted for clarity, and selected bond distances and angles are listed in Table 4. The $[LaNi_2(tam)_2]^+$ cation contains an eight-coordinate La(III) ion bonded to two $[tam]^{3-}$ ligands, each of which is tridentate with respect to the La(III) ion and hexadentate with respect to one Ni(II) ion. Each $[tam]^{3-}$ ligand encapsulates a Ni(II) ion via its three amine and three phenolato functions, rendering each Ni(II) coordination sphere approximately octahedral. All six phenols are deprotonated and

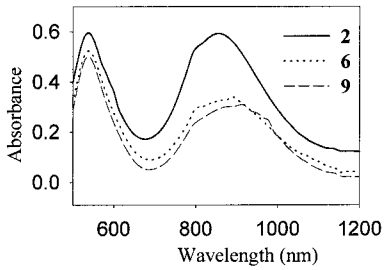

Figure 6. UV/vis spectra of **2**, **6**, and **9** in CH_2Cl_2.

form bridging bonds between the Ni(II) and La(III) ions. Two solvent molecules [one being water (O(7)) and the second being water (O(8d)), methanol, or ethanol (O(3))] occupy the remaining coordination sites on the lanthanum(III) ion. The $[LaNi_2(tam)_2(CH_3OH)_{1/2}(CH_3CH_2OH)_{1/2}(H_2O)]^+$ cation is not linear. A detailed shape analysis[26] determined that the geometry of the La(III) ion is best described as a D_{4d} square antiprism, distorted toward a C_{2v} bicapped octahedron. The Ni−La distances are 3.1900(7) Å (La(1)−Ni(1)) and 3.1533(7) Å (La(1)−Ni(2)), which are shorter than previously observed in other Ni−La systems, such as the tren-based amine phenol La/Ni system described by Archibald et al. where Ni−La = 3.355(5) Å.[27] The average La−O(ligand) bond lengths (2.519 Å) are in good agreement with other crystallographically characterized examples of the ligand $[tam]^{3-}$. The average Ni−O bond lengths (2.075(3) Å for Ni(1) and 2.078(3) Å for Ni(2)) are slightly longer and the average Ni−N bond lengths (2.082(4) Å for Ni(1) and 2.081(4) Å for Ni(2)) are slightly shorter than observed in the parent complex (**1**) (average $Ni-O_{(phenoxy)}$ = 2.035(3) Å and Ni−N(ligand) = 2.0767(4) Å). This was to be expected, since the acidic lanthanide(III) ion will withdraw electron density from the $[Ni(tam)]^-$ moiety.[28] This will have a two-fold effect: First, the Ni−O bonds will be slightly lengthened since the phenolato groups become bridging. Second, the trans amino groups will be pulled closer to the Ni(II) ion, and hence their bond lengths to Ni will be shortened. The fact that the two nickel centers in **2** are in comparable environments is also reflected by the UV/vis spectrum (see Figure 6), which indicates that there is no splitting in either the 860 nm (ν_1, $^3A_{2g} \rightarrow {}^3T_{2g}$, ϵ = 147 M^{-1} cm^{-1}) or the 540 nm (ν_2, $^3A_{2g} \rightarrow {}^3T_{1g}$, ϵ = 122 M^{-1} cm^{-1}) absorptions.[29] The ν_3 band for all of these compounds, however, was not observed, being obscured by a very strong charge-transfer band at 285 nm ($\epsilon = 3.9 \times 10^4$ M^{-1} cm^{-1}). The particular Ni−Ln−Ni (Ln = La in this case) arrangement found in this series of compounds is very similar to that found in a series of linear thiophenolate-bridged heterotrinuclear transition metal complexes reported very recently.[30]

(d) $[DyNi_2(tam)_2(CH_3OH)(H_2O)]ClO_4 \cdot CH_3OH \cdot H_2O$ (6). The structure of the $[DyNi_2(tam)_2]^+$ cation in **6** shares some similarities with its La(III) analogue (**2**). The cation, which has C_1 symmetry, contains a Dy(III) ion with two $[Ni(tam)]^-$ units coordinated to it. The Dy(III) ion is seven-coordinate, being coordinated by two $[Ni(tam)]^-$ complex ligands, one bidentate

(26) (a) Porai-Koshits, M. A.; Aslanov, L. A. *Zh. Strukt. Khim.* **1972**, *13*, 266. (b) Muetterties, E. L.; Guggenburger, L. J. *J. Am. Chem. Soc.* **1974**, *96*, 1748.
(27) Archibald, S. J.; Blake, A. J.; Parsons, S.; Schröder, M. *J. Chem. Soc., Dalton Trans.* **1997**, 173.
(28) Templeton, D. H.; Dauben, C. H. *J. Am. Chem. Soc.* **1954**, *76*, 5237.
(29) Lever, A. B. P., *Inorganic Electronic Spectroscopy*, Elsevier: New York, 1984.
(30) (a) Glaser, T.; Beissel, T.; Bill, E.; Weyhermüller, T.; Schünemann, V.; Meyer-Klaucke, W.; Trautwein, A. X.; Wieghardt. K. *J. Am. Chem. Soc.* **1999**, *121*, 2193. (b) Glaser, T.; Bill, E.; Weyhermüller, T.; Meyer-Klaucke, W.; Wieghardt. K. *Inorg. Chem.* **1999**, *38*, 2632.

and one tridentate (vide infra). Each $[tam]^{3-}$ ligand encapsulates a Ni(II) ion metal via its three amine and three phenolato functions, which results in each Ni(II) ion having approximately octahedral geometry. All of the phenolato functions are deprotonated; only five of them, however, bridge between the Ni(II) and Dy(III) ions. One of the phenolato O atoms (O(6)) has a very long interaction (Dy(1)−O(6) = 3.197(3) Å) and hence is not formally bonded to the Dy(III) ion. One methanol and one water molecule occupy the remaining coordination sites on the dysprosium(III) ion. The $DyNi_2$ cation is not linear. A detailed shape analysis[26] determined that the geometry of the Dy(III) ion was best described as capped trigonal prismatic.

The average Ni−Dy distance is 3.1338(7) Å (e.g., Dy(1)−Ni(1) = 3.0134(7) Å and Dy(1)−Ni(2) = 3.2542(7) Å), which is shorter than one would expect by comparison with the $LaNi_2$ analogue (cf. average La−Ni = 3.1717(7) Å). This can be explained upon closer inspection of the relevant Ln−O bond lengths and Ln−O−Ni angles. From Tables 4 and 5, it can be seen that the corresponding La−O bond distances are significantly longer than those of Dy−O [e.g., La(1)−O(4) = 2.410(3) Å and La(1)−O(2) = 2.472(3) Å, while Dy(1)−O(4) = 2.267(3) Å and Dy(1)−O(2) = 2.273(4) Å], which obviously results from the lanthanide contraction (ionic radii for La^{3+} and Dy^{3+} (both CN = 8) are 1.216 and 1.027 Å, respectively[31]). On the other hand, the corresponding Ni−O bond distances and Ln−O−Ni angles are comparable. The Dy−O(ligand) bond lengths show no significant differences between the halves of the molecule. The average bond length is 2.275(4) Å, normal for Dy−O bonds.

The average Ni−O bond lengths within each $[Ni(tam)]^-$ moiety are significantly different. The average Ni(1)−O bond length is 2.066(4) Å, while the average Ni(2)−O bond length is 2.082(4) Å. The average Ni−N bond lengths also show the same trend (average Ni(1)−N = 2.063(4) and average Ni(2)−N = 2.082(4) Å). Even though it is a fact that the Ni−O and Ni−N bond distances in both nickel centers are within expected values, the shorter Ni(1)−O and Ni(1)−N bond distances might suggest that the better bridging between Dy and Ni(1) via three phenolato oxo groups (O(1), O(2), O(3)) creates a better coordination environment for Ni(1). The difference in coordination environment between these two nickel centers is shown in the UV/vis spectrum of **6** (see Figure 6), in which the band ν_1 ($^3A_{2g} \rightarrow {}^3T_{2g}$) at ca. 850 nm is obviously split.

(e) $[YbNi_2(tam)_2(H_2O)]ClO_4 \cdot 2.58H_2O$ (9). The $[YbNi_2(tam)_2(H_2O)]^+$ cation in complex **9** was found to be very similar in the solid state to the Dy(III) analogue. The C_1 symmetry cation contains an Yb(III) ion with two $[Ni(tam)]^-$ units coordinated to it. The Yb(III) ion in **9** has a typical six-coordination sphere with a distorted octahedral geometry, being bonded to two $[Ni(tam)]^-$ ligands. As in **6**, one $[Ni(tam)]^-$ is tridentate and the other bidentate with respect to Yb(III); the sixth coordination site is occupied by a water molecule. All of the phenolato functions are deprotonated; only five of them, however, are bridging between the Ni(II) and Yb(III) ions. One of the phenolate O atoms is not bonded to the Yb(III) ion. Each $[tam]^{3-}$ ligand encapsulates a Ni(II) ion via its three amine and three phenolato functions; hence, each nickel(II) ion has approximately octahedral geometry. The distances between Ni(II) and Yb(III) are 2.9081(8) Å (Yb(1)−Ni(1)) and 3.2702(7) Å (Yb(1)−Ni(2)), which are comparable to the distances between Dy and Ni in **6**. The Yb−O bond lengths, average of 2.212(4) Å for the Ni(1) ligand and 2.196(4) Å for the Ni(2) ligand, are significantly longer than the corresponding Dy−O distances in **6** (an obvious result of the lanthanide contraction effect − ionic radius of Yb^{3+} (CN = 7) is only 0.925 Å[31]). The corresponding Ni−O and Ni−N bond lengths, however, are very similar to those in **6** and also show differences when their values within each $[Ni(tam)]^-$ moiety are compared, which is illustrated by the split bands in the UV/vis spectrum of **9** (see Figure 6).

The majority of prior studies into the coaggregation of metal ions have generally involved only two metal ions.[27,32] Cases where more than two metal ions have been assembled into novel complexes have largely been fortuitous, since the resultant complexes are generally the result of oligomerization of a simpler species with a ligand (or counterion) that has a capacity to bridge.[33] In our system, however, the approach taken was to build lanthanides into a construct where the precursor transition metal complex of the encapsulated type in Chart 1 acts as a ligand for a Ln(III) ion in a bicapped fashion. This design has successfully generated complexes that contain novel architectures, wherein $[Ni(tam)]^-$ caps a lanthanide(III) ion. This approach in itself is not novel; the fact that two $[Ni(tam)]^-$ units cap the lanthanide is. This type of arrangement has not been observed previously for amine phenol ligands. It has, however, been observed for Schiff base ligands, which have less flexibility, resulting in greater 3d−4f distances.[34]

Magnetic Properties. Magnetic susceptibilities were measured on powdered samples of **2**, **6**, and **9** at an applied field of 10 000 G over the temperature range 2−300 K. The results are shown as plots of effective magnetic moment (on a per mole of $LnNi_2$ basis) versus temperature in Figure 7. The lanthanide in **2** is diamagnetic (La(III), $S = 0$), and hence the magnetization in this sample arises solely from the Ni(II) ($S = 1$) ions. The Ni(II) ions are octahedrally coordinated and are expected, therefore, to exhibit spin-only moments modified by the effects of second-order spin−orbit coupling, which leads to a g value in excess of 2.[35] The value of μ_{eff} at 300 K is 4.44 μ_B, corresponding to two Ni(II) ions with μ_{eff}(per Ni) = μ_{Ni} = 3.14 μ_B and $g = 2.22$. The moment decreases only marginally from 300 to 10 K, below which a rather sharp drop due to the effects of zero-field splitting is seen (Figure 7). In summary, the magnetic behavior of **2** is consistent with the presence of two magnetically isolated octahedral Ni(II) centers.

(31) Shannon, R. D., *Acta Crystallogr., Sect. A* **1976**, *32*, 751.

(32) (a) Ramade, I.; Kahn, O.; Jeannin, Y.; Robert, F. *Inorg. Chem.* **1997**, *36*, 930. (b) Piguet, C.; Rivara-Minten, E.; Bernardinelli, G.; Bunzli, J.-C. G.; Hopfgartner, G. *J. Chem. Soc., Dalton Trans*. **1997**, 421. (c) Costes, J.-P.; Dahan, F.; Dupuis, A.; Laurent, J. P. *Inorg. Chem.* **1996**, *35*, 2400. (d) Wang, S.; Pang, Z.; Smith, K. D. L.; Hua, Y.; Deslippe, C.; Wagner, M. J. *Inorg. Chem.* **1995**, *34*, 908. (e) Chen, L.; Breeze, S. R.; Rousseau, R. J.; Wang, S.; Thompson, L. K. *Inorg. Chem.* **1995**, *34*, 454. (f) Benelli, C.; Blake, A. J.; Milne, P. E. Y.; Rawson, J. M.; Winpenny, R. E. P. *Chem.—Eur. J.* **1995**, *1*, 614. (g) Benelli, C.; Fabretti, A. C.; Giusti, A. *J. Chem. Soc., Dalton Trans* **1993**, 409.

(33) (a) Yukawa, Y.; Igarashi, S.; Yamano, A.; Sato, S. *J. Chem. Soc., Chem. Commun.* **1997**, 711. (b) Brechin, E. K.; Harris, S. G.; Parsons, S.; Winpenny, R. E. P. *J. Chem. Soc., Dalton Trans*. **1997**, 1665. (c) Sanz, J. L.; Ruiz, R.; Gleizes, A.; Lloret, F.; Faus, J.; Julve, M.; Borrás-Almenar, J. J.; Jouraux, Y. *Inorg. Chem.* **1996**, *35*, 7384. (d) Oushoorn, R. L.; Boubekeur, K.; Batail, P.; Guillou, O.; Kahn, O. *Bull. Soc. Chim. Fr*. **1996**, *133*, 777. (e) Blake, A. J.; Cherepanov, V. A.; Dunlop, A. A.; Grant, C. M.; Milne, P. E. Y.; Rawson, J. M.; Winpenny, R. E. P. *J. Chem. Soc., Dalton Trans*. **1994**, 2719. (f) Andruh, M.; Ramade, I.; Codjovi, E.; Guillou, O.; Kahn, O.; Trombe, J. C. *J. Am. Chem. Soc*. **1993**, *115*, 1822. (g) Guillou, O.; Bergerat, P.; Kahn, O.; Bakalbassis, E.; Boubekeur, K.; Batail, P.; Guillot, M. *Inorg. Chem.* **1992**, *31*, 110.

(34) (a) Cu−Gd = 3.367 Å: Bencini, A.; Benelli, C.; Caneschi, A.; Carlin, R. L.; Dei, A.; Gatteschi, D. *J. Am. Chem. Soc*. **1985**, *107*, 8128. (b) Cu−Gd = 3.347 Å: Bencini, A.; Benelli, C.; Caneschi, A.; Dei, A.; Gatteschi, D. *Inorg. Chem.* **1986**, *25*, 572.

(35) Figgis, B. N. *Introduction to Ligand Fields*; Interscience: New York, 1966.

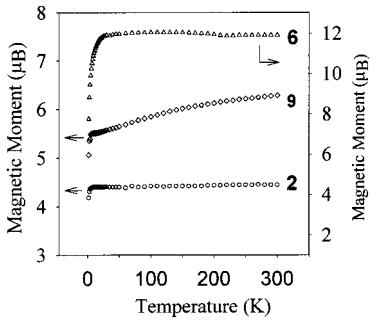

Figure 7. Temperature dependence of the magnetic moments of **2**, **6**, and **9** shown on a per mole of $LnNi_2$ basis.

The magnetic moment of **6** at 300 K is 11.9 μ_B. This moment, μ_{DyNi_2}, arises from the contributions of one Dy(III) ion and two Ni(II) ions. Assuming $\mu_{Ni} = 3.14$ μB (as determined for **2**) and employing eq 1, we calculate $\mu_{Dy} = 11.0$ μ_B as the contribution

$$\mu_{DyNi_2} = (\mu_{Dy}{}^2 + 2\mu_{Ni}{}^2]^{1/2} \quad (1)$$

from the Dy(III) ion. This value is in excellent agreement with the value of 10.6 μ_B calculated from the formula $\mu_J = g[J(J+1)]^{1/2}$ for the $^6H_{15/2}$ ground state of Dy(III). Because of low ligand field potentials and strong spin−orbit couplings in the case of lanthanide ions, this formula is expected to apply to Dy(III).[35] The magnetic moment of **6** remains essentially constant from 300 to about 22 K, below which it decreases to a low of 7.76 μ_B at 2 K. This decrease in moment at low temperatures is in part due to zero-field splitting of Ni(II) as seen for **2**; however, the effect is much too large to be due only to this phenomenon. Employing the values 2.96 μ_B for μ_{Ni} at 2 K (obtained from the 2 K data for **2**) and 11.0 μ_B for μ_{Dy}, we calculate $\mu_{DyNi_2} = 11.8$ μ_B, a value far in excess of the observed 7.76 μ_B. This observation and the fact the temperature dependence of the moment in **6** extends over a slightly larger temperature range than that seen for **2** suggest there may be some antiferromagnetic coupling in the former compound. Any coupling must, however, be weak since only very low temperature data are affected by it.

The magnetic moment of **9**, μ_{YbNi_2}, is 6.28 μ_B at 300 K. Employing 3.13 μ_B for μ_{Ni}, as above, we calculate $\mu_{Yb} = 4.44$ μ_B. This compares with the theoretical $\mu_J = 4.50$ μ_B for the $^2F_{7/2}$ ground state of Yb(III). In contrast to the situation for **2** and **6**, the magnetic moment of **9** decreases measurably on lowering the temperature over the entire range of temperatures studied. It varies from 6.28 μ_B at 300 K to 5.50 μ_B at 7 K (Figure 7). Below 7 K, the rapid drop in moment to 5.06 μ_B at 2 K is, as before, at least partly due to zero-field splitting in Ni(II). The temperature variation of the magnetic moment of **9** over the range 300−7 K provides clear evidence of antiferromagnetic exchange between the Yb(III) and the Ni(II) ions in this compound. The exchange coupling in **9** is stronger than that in **6**, leading to the general conclusion that the strength of d^n-f^n coupling between Ni(II) and lanthanide ions is determined, at least in part, by the size of the lanthanide ion, increasing with decreasing size. Further examples are needed to confirm this. Unfortunately, we are unaware of a theoretical treatment of a system such as this one that would allow us to model the behavior in order to obtain a quantitative result for the strength of the exchange interaction. The nature of the d^n-f^n interactions observed here contrasts with that reported for the Cu(II)−Ln(II) systems, where either antiferromagnetic or ferromagnetic exchange may be observed depending on the f^n configuration.[36,37]

Conclusions

The greater geometric flexibility of amine phenol ligands, as compared to their Schiff base analogues, allowed for the formation of coaggregated d- and f-block metal ion complexes. This was highlighted by the stabilization of complexes of the type $[LnM_2L_2]^+$ having a range of lanthanide(III) ions by the ligand tam^{3-} (M = Ni(II) in this paper; studies of other first-row transition metal ions are in progress). The solid-state structures of three of these complexes revealed that the ligand tam^{3-} encapsulated Ni(II) ions in an octahedral geometry, resulting in the formation of a $[Ni(tam)]^-$ moiety which could be incorporated as a ligand for lanthanide(III) ions. The choice of counterion was critical in determining the nature of the resulting complex; the bicapped $[LnM_2(tam)_2]^+$ units were only isolated if perchlorate was employed. When a more strongly coordinating counterion, such as NO_3^-, was chosen the resulting complex was a capped species, i.e., $[ErNi(tam)(NO_3)_3]^-$.[38] Variable-temperature magnetic studies indicated that antiferromagnetic exchange coupling between Ni(II) and a lanthanide ion increased with decreasing size of the lanthanide ion.

Acknowledgment. We gratefully acknowledge the NSERC (Canada) for the provision of operating grants (R.C.T., C.O.), the EPSRC (U.K.) for support of the crystallography unit (M.B.H.), and Dr. P. Caravan for helpful discussions.

Supporting Information Available: Complete tables of crystallographic data, atomic coordinates, *U*(eq) values, bond lengths, bond angles, anisotropic thermal parameters, hydrogen atom coordinates, torsion angles, nonbonded contacts, and least-squares planes. This material is available free of charge via the Internet at http://pubs.acs.org.

IC991171B

(36) Andruh, M.; Ramade, I.; Codjovi, E.; Guillou, O.; Kahn, O.; Trombe, J. C. *J. Am. Chem. Soc.* **1993**, *115*, 1822.
(37) Costes, J.-P.; Dahan, F.; Dupuis, A.; Laurent, J.-P. *Chem.—Eur. J.* **1998**, *4*, 1616.
(38) Read, P. W.; Orvig, C. Unpublished results.